Nonlinear optical absorption in silver nanosol

Nonlinear optical absorption in silver nanosol

K P Unnikrishnan[1]**, V P N Nampoori**[1]**, V Ramakrishnan**[2]**,
M Umadevi**[2] **and C P G Vallabhan**[1]

[1] International School of Photonics, Cochin University of Science & Technology,
Cochin 682022, India
[2] School of Physics, Madurai Kamaraj University, Madurai 625021, India

E-mail: kpu@cusat.ac.in

Abstract
Nonlinear optical absorption in silver nanosol was investigated at selected
wavelengths (456 nm, 477 nm and 532 nm) using open aperture Z-scan
technique. It was observed that nature of nonlinear absorption is sensitively
dependent on input fluence as well as on excitation wavelength. Besides, the
present sample was found to exhibit reverse saturable absorption (RSA) and
saturable absorption (SA) at these wavelengths depending on excitation
fluence. RSA is attributed to enhanced absorption resulting from
photochemical changes. SA observed for fluence values lower and higher
than those corresponding to RSA are, respectively, attributed to plasmon
bleach and saturation of RSA.

1. Introduction

Most of the optical properties of metal nanoparticles are
different from those of bulk materials because of the dielectric
and quantum confinement effects, which arise due to reduction
in particle size down to nanometer range. The quantum
confinement gives rise to discrete energy levels in an otherwise
continuous band. However, such effects are significant only if
the particle size is of the order of sub-nanometre (<1 nm).
On the other hand, dielectric confinement effects can be
observed even in particles of bigger size. In the case of
metals, when particle size is reduced, the plasmon peak of
the bulk (usually in the deep UV region) gets down shifted
in energy to visible or near UV region. This leads to
the formation of characteristic surface palsmon resonance
(SPR) band [1–4]. SPR is collective mode of oscillations
of free electrons in the conduction band. Most of the
optical properties of nanoparticles are due to SPR. Although
in the dipole approximation SPR band is independent of
the particle size, it has been found that the peak position
and width of SPR band depend on the particle size as well
as on their shape and environment [5]. Mie theory and
Maxwell–Garnet theory explain SPR band in terms of higher
moment oscillations and particle size [6]. Nanoparticles have
been suggested for a number of applications in photonic
technology such as optical limiting [7], ultrafast switching
[8] and data storage [9]. Nanoparticles are widely used

in surface enhanced Raman scattering [10] as well as in
the study of liquid–metal interface [11]. In most of these
applications, nonlinear optical (NLO) effects play a major role.
Hence, study of NLO properties of nanoparticles becomes
vitally important. Amongst the nanoparticles studied by
earlier researchers at 532 nm, nonlinear absorption and optical
limiting properties were found to be higher in silver and
silver containing nanomaterials [12, 13]. Degenerate four
wave mixing (DFWM) studies in Ag nanoparticles in solution
[14] as well as in glass matrix [15] and also in colloidal gold
[16] have been reported. There are also reports on second
harmonic generation (SHG) in gold nanoparticles [17, 18]. In
this paper, we report nonlinear absorption in silver nanosol
at three selected wavelengths in the red region of the SPR
peak using nanosecond pulses. Selected wavelengths include
456 nm (inside SPR), 477 nm (on the edge of SPR) and 532 nm
(outside the SPR).

2. Experimental

In a typical open aperture Z-scan experiment, the transmittance
$T(z)$ of the sample is measured as the sample is moved along
the propagation direction (z) of a focussed gaussian laser beam.
The plot thus obtained [$T(z)$ vs z] is normalized with respect to
$T(z)$ for large values of $|z|$. The measurements at 532 nm were
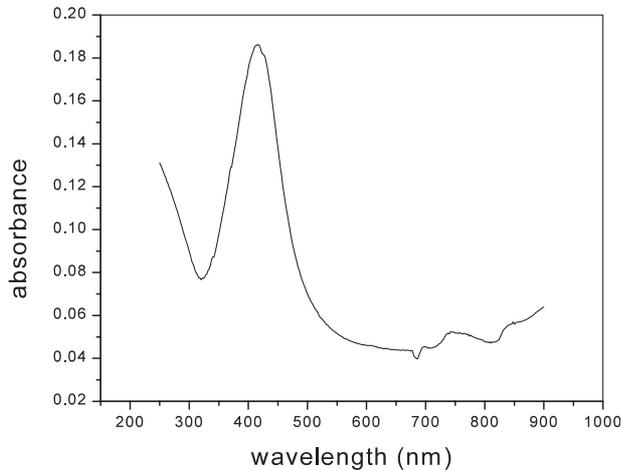made with second harmonic of a Nd : YAG laser (pulse width

Figure 1. Absorption spectrum.

≈ 7 ns), while measurements at the other wavelengths (456 nm and 477 nm) were made using a MOPO (Spectra Physics 710, pulse width 4 ns). Incident and transmitted energies were measured using photodiodes and were averaged over hundred shots using a digital storage oscilloscope (Tektronix 360). Beam waist at focus ω_0 and Rayleigh range z_0, both in the sample, varied from 11 μm to 14 μm and 1 mm to 1.4 mm, respectively, depending on the wavelength of excitation.

Silver nanosol was prepared by standard reduction technique. Ten millilitres of 1 mM AgNO$_3$ solution was added drop wise to 30 ml of 2.0 mM NaBH$_4$ solution. The solution was constantly stirred well. Absorption spectrum of the sample was taken with a spectrophotometer (JASCO V 570) and is shown in figure 1. SPR peak of the sample (nanosol) occurs at 416 nm.

3. Results and discussion

Electron dynamics in noble metal nanoparticles such as Ag and Au following laser excitation has been studied in detail [5, 6, 10, 19]. Results of those investigations are relevant in the context of present measurements. When nanoparticles are irradiated, the SPR band gets excited, which leads to the dipole and higher order (quadrupole, octopole etc) oscillations. These oscillations can couple with the applied electric field. Consequently, SPR frequency of excited atoms differs from that of unexcited atoms. Therefore, SPR band cannot further absorb in the original SPR band region. This leads to SPR bleach [19]. Bleaching of the absorption, which occurs in ultrafast timescale, is accompanied by the appearance of broad transient absorption on both red and blue side of the bleached region. The excited electrons have an energy higher than Fermi energy and hence, they are called hot electrons. The hot electrons get thermalized by dissipating excess energy through successive processes of electron–surface scattering, electron–electron scattering and electron–phonon scattering [3]. Exact timescales of all these processes may vary according to the type and environment of nanoparticles. At the end of thermalization process, heat energy is transferred to the surrounding medium, viz, the solvent in the case of nanoparticle solutions and the substrate in the case of nanoparticle films. This excess thermal energy will increase the temperature of surrounding medium, which in turn influence the SPR. Full recovery of plasmon bleach is delayed and transient absorption is observed till thermalization of hot electrons is complete. The electron–electron scattering is very fast and occurs in sub-picosecond timescale. Depending on the experimental conditions, the broad transient absorption may consist of two components of different timescales, viz, a fast picosecond component and a comparatively slow one, lasting for a few nanoseconds. In gold nanoparticles, recovery of plasmon band takes place in a timescale slightly greater than 50 ps with a single exponential fit [6]. However, in silver nanoparticles transient absorption satisfies a double exponential fit, which consists of fast (100 ps) and slow (1.5 ns) components. Transient absorption spectra measurements on silver nanoparticles have shown that though strong bleaching of the plasmon band occurs in sub-nanosecond timescale, complete recovery of plasmon bleach is delayed up to a few nanoseconds ($\cong 2$ ns) [19].

The component of transient absorption taking place in nanosecond timescale is mainly due to photochemical change induced absorption arising from photo-ejection of electrons from the sample on laser irradiation. Photo-ejection of electrons is a multi photon process. The ejected electrons can charge the nanoparticle surface electrically, leading to aggregation, which results in a transient state (Ag$^+$e$^-$) generated by photo induced intraparticle charge separation [19]. During this transient period, aggregation may also result in the formation of large nanoparticles clusters with very broad plasmon band. The whole process takes place in nanosecond timescale. These phenomena result in transient absorption. Besides, ejection of electrons creates holes, which can act as free carriers giving rise to free carrier absorption (FCA). It may thus be noted that slow component (ns) of transient absorption is due to FCA and photochemical change induced absorption occurring in the sample while the fast (ps) component is due to thermalization of hot electrons. Optical limiting property observed under nanosecond excitation, in silver as well as in silver halides nanoparticles [12, 13] are explained taking in to account the slow component. It may be noted that in the case of silver nanoparticles interband transitions from filled d-states to upper Fermi levels occur in the UV region (above 4 eV) and hence, the complications arising from interband transitions in nonlinear response can be neglected to a good approximation.

In nanoparticle systems, nonlinear scattering, which is a size dependent mechanism, is an alternative process that can mimic nonlinear absorption. Optical limiting due to nonlinear scattering has been reported in gold nanoparticles [20]. Fluence dependent switching between saturable absorption (SA) and reverse saturable absorption (RSA) observed in the present investigation indicates that nonlinear scattering is very unlikely in the present case. In this context, it is very relevant to point out that strong optical limiting property due to nonlinear scattering has been reported in carbon black suspension (CBS). In CBS, optical limiting is due to nonlinear scattering by microplasma generated at the focal region [21, 22]. The results obtained in the present experiment will be explained taking into account the SPR band bleach, absorption due to photochemical changes as well as a possible particle size-selective excitation.

Plots (a) and (b) in figure 2 shows the open aperture Z-scan curves obtained at 532 nm for fluence values (at
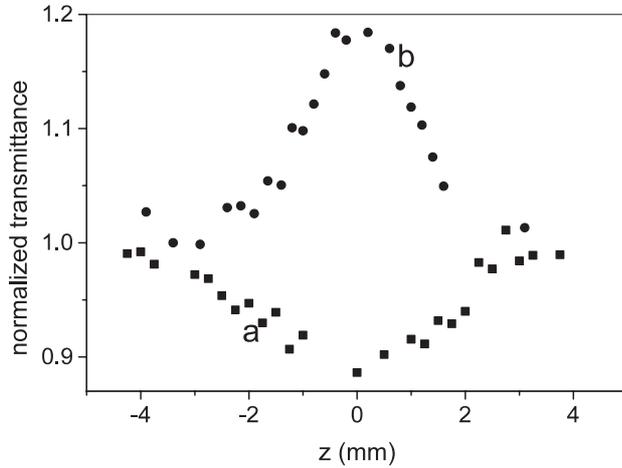
Figure 2. Open aperture Z-scan curve at 532 nm: (a) 0.08 J cm^{-2}; (b) 0.5 J cm^{-2}.
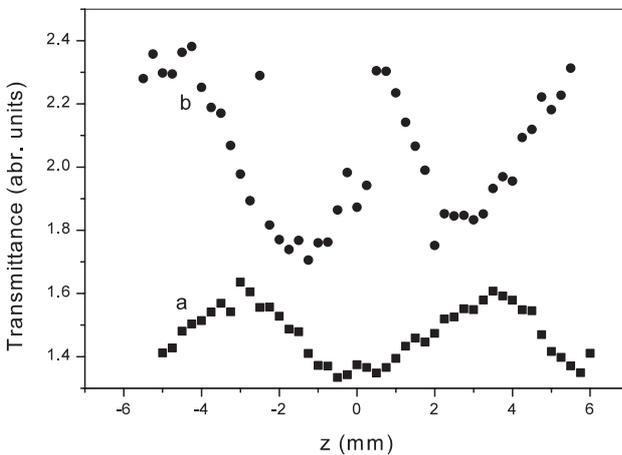

Figure 4. Open aperture Z-scan curve at 456 nm: (a) 0.1 J cm^{-2}; (b) 0.2 J cm^{-2}; (c) 0.6 J cm^{-2}.

Figure 3. Open aperture Z-scan curve at 477 nm: (a) 0.08 J cm^{-2}; (b) 0.44 J cm^{-2}.

focus) of 0.08 J cm^{-2} and 0.5 J cm^{-2}, respectively. Plot (a) corresponds to RSA, whereas plot (b) indicates SA. Obviously, as energy is increased RSA changes to SA. RSA (plot (a) in figure 2) can be due to enhanced absorption resulting from photochemical changes. FCA is also an alternative mechanism for RSA. However, since the present system of nanoparticles is uncapped, photochemical change induced absorption is very likely phenomenon. Since SA is observed for fluence values higher than those corresponding to RSA, it is attributed to saturation of RSA [23].

Figure 3 shows the open aperture Z-scan curves obtained at 477 nm for fluence values (at focus) of 0.08 J cm^{-2} and 0.44 J cm^{-2}. In Z-scan experiments, fluence is a maximum at the focus and it continuously decreases in regions away from the focus. Therefore, plot (a) figure 3 indicates that for lower values of fluence, sample exhibits SA but as fluence is increased SA changes to RSA. Here, SA takes place for lower values of fluence than those corresponding to RSA and hence, SA observed in this case is of different origin from the case of 532 nm. In the present case, SA can be due to SPR bleach [24]. RSA, as in the case of 532 nm, is attributed to photochemical change induced absorption. Each point in plot (b) of figure 3
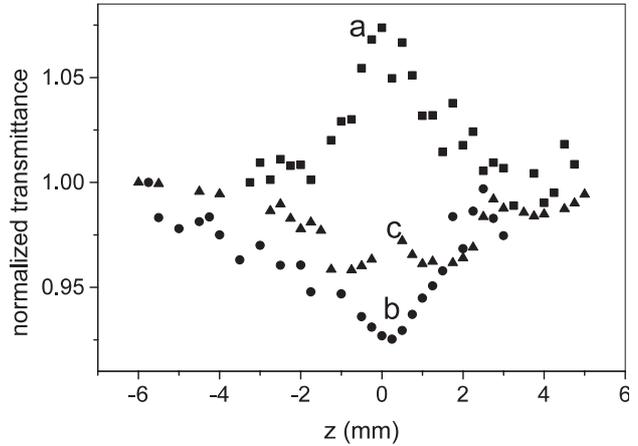
corresponds to a fluence value, about five times higher than that of plot (a). It is interesting to note that plot (b) is a mirror image of plot (a). SA observed in plot (b) around the focus occurs for higher fluence values, after the observation of RSA. Hence, it arises due to saturation of RSA. From figure 3 it is evident that both the SA and RSA are very sensitively dependent on input fluence. Hence, the plots in figure 3 were not normalized to linear transmittance. Plots (a), (b) and (c) of figure 4 show the open aperture Z-scans curves obtained at 456 nm for input fluence (at focus) of 0.1 J cm^{-2}, 0.2 J cm^{-2} and 0.6 J cm^{-2}, respectively. SA in plot (a) of figure 4, which corresponds to lower values of fluence than those corresponding to RSA can be due to plasmon bleach. When fluence is increased to 0.2 J cm^{-2} SA changes to RSA, which can be attributed to photochemical change induced absorption. When fluence is further increased to 0.6 J cm^{-2} a clear sign of emergence of SA is observed at focus, which can be due to saturation of RSA.

A comparison of figures 2–4 give important results. They are (1) no plasmon bleach was observed at 532 nm; 532 nm is outside the SPR band and hence, probability for plasmon bleach can be less, (2) dynamic range of RSA for 456 and 532 nm are nearly same but it is very less for 477 nm; (3) threshold level for plasmon bleach, as well as for RSA is very low at 477 nm in comparison with 456 nm. Observed lower threshold for plasmon bleach at 477 nm may be explained if we assume that there is close correspondence between SPR band and number density of particles with specific size. Particle size-selective excitation in nanoparticles has been previously reported. Number density of nanoparticles that are excited at 456 nm can be higher than those excited at 477 nm. Consequently, number of photons (greater fluence) may be required for plasmon bleach at 456 nm. The reason for very low threshold as well as dynamic range of RSA at 477 nm is not clear from the present measurements. Further studies may be required in this direction.

4. Conclusion

Nonlinear absorption in silver nanosol was studied at a number of selected wavelengths 456 nm (inside the SPR band) 477 nm (on the edge of SPR) and 532 nm (outside the SPR band). It was

observed that (1) nature of nonlinear absorption is a sensitive to intensity and wavelength of excitation and (2) that the sample can act as a saturable absorber as well as reverse saturable absorber at the same wavelength depending on the excitation intensity. The results were explained taking into account the SPR bleach, photochemical changes and a possible particle size-selective excitation effect. Threshold fluence level and dynamic range of RSA at 477 nm, which happens to be on the edge of SPR, were found to be much lower than those of other two wavelengths.

It may be appropriate to point out that the present measurements have been made with a nanosecond laser source and hence, time-resolved studies were not possible within the scope and context of this paper. Therefore, our attempt has been to give very likely interpretation for the present results on the basis of the results of time-resolved studies carried out by other researchers on similar samples [19]. However, a time-resolved study is required to understand the exact processes taking place in the sample on laser irradiation. We plan to carry out a detailed time-resolved study in silver nanosol at future date.

Acknowledgment

References

[1] Schmid G and Chi L F 1998 *Adv. Mater.* **10** 515–26
[2] Del Fatti N, Vallee F, Flytzanis C, Hamanaka Y and Nakamura A 2000 *Chem. Phys.* **251** 215–26
[3] Bigot J Y, Halte V, Merle J C and Daunois A 2000 *Chem. Phys.* **251** 181–203
[4] Stagira S, Nisoli M, De Silvestri S, Stella A, Tognini P, Cheyssac P and Kofman R 2000 *Chem. Phys.* **251** 259–67
[5] Link S, Burda C, Wang Z L and El-Sayed M A 1999 *J. Chem. Phys.* **111** 1255–64
[6] Ahmadi T S, Logunov S L and El-Sayed M A 1996 *J. Phys. Chem.* **100** 8053–6
[7] Sahyun M R V, Hill S E, Serpone N, Danesh R and Sharma D K 1996 *J. Appl. Phys.* **79** 8030–7
[8] Inouye H, Tanaka K, Tanahashi I and Nakatsuka H 2000 *Japan. J. Appl. Phys.* **39** 5132–3
[9] Ditlbacher H, Krenn J R, Lamprecht B, Leitner A and Aussenegg F R 2000 *Opt. Lett.* **25** 563–5
[10] Shuming Nie and Emory S R 1997 *Science* **275** 1102–6
[11] Roberti T W, Smith B A and Zhang J Z 1995 *J. Chem. Phys.* **102** 3860–6
[12] Han M Y, Huang W, Chew C H and Gan L M 1998 *J. Phys. Chem.* B **102** 1884–7
[13] Ya Ping Sun, Riggs J E, Rollins H W and Gurudu R 1999 *J. Phys. Chem.* B **103** 77–82
[14] Faccio D, Di Trapani P, Borsella E, Gonella F, Mazzoldi P and Malvezzi A M 1998 *Europhys. Lett.* **43** 213–18
[15] Uchida K, Kaneko S, Omi S, Hata C, Tanji H, Asahara Y, Ikushima A J, Tokizaki T and Nakamure A 1994 *J. Opt. Soc. Am.* B **11** 1236–43
[16] Bloemer M J, Haus J W and Ashley P R 1990 *J. Opt. Soc. Am.* B **7** 790–5
[17] Antoine R, Brevet P F, Girault H H, Bethell D and Schiffrin D J 1997 *Chem. Commun.* 1901–2
[18] Antoine R, Pellarin M, Palpant B, Broyer M, Prevel B, Galletto P, Brevet P F and Girault H H 1998 *J. Appl. Phys.* **84** 4532–6
[19] Kamat P V, Flumiani M and Hartland G V 1998 *J. Phys. Chem.* B **102** 3123–8
[20] Francois L, Mostafavi M, Belloni J, Delouis J F, Delaire J and Feneyrou P 2000 *J. Phys. Chem.* B **104** 6133–7
[21] Mansour K, Soileau M J and Stryland E W V 1992 *J. Opt. Soc. Am.* B **9** 1100–9
[22] Ya Ping, Riggs J E, Henbest K B and Martin R B 2000 *J. Non. Opt. Phys. Mater.* **9** 481–503
[23] Deng X, Zhang X, Wang Y, Song Y, Liu S and Li C 1999 *Opt. Commun.* **168** 207
[24] Philip R, Kumar G R, Sandyarani N and Pradeep T 2001 *Phys. Rev.* B **62** 1360–6